Supplementary Information

Perovskite solar cells approaching 25% using side chain terminated hole transport materials with low concentration in non-halogenated solvent process

Zhiqing Xie,‡[ac] Yeongju Do,‡[a] Seung Ju Choi,‡[bc] Ho-Yeol Park,[a] Hyerin Kim,[a] Jeonghyeon Kim,[a] Donghyun Song,[a] Thavamani Gokulnath,[a] Hak-Beom Kim,[b] In Woo Choi,[b] Yimhyun Jo,[b] Dong Suk Kim,*[d] Seog Young Yoon,*[c] Young-Rae Cho,*[c] and Sung-Ho Jin*[a]

[a]Department of Chemistry Education, Graduate Department of Chemical Materials, Institute for Plastic Information and Energy Materials, Sustainable Utilization of Photovoltaic Energy Research Center/Engineering Research Center, Pusan National University, Busan 46241, Republic of Korea.

[b]Advanced Center for Energy R&D Center, Korea Institute of Energy Research (KIER), Ulsan, Republic of Korea.

[c]Division of Materials Science and Engineering, Pusan National University, Busan 46241, Republic of Korea.

[d]Graduated School of Carbon Neutrality, Ulsan National Institute of Science and Technology(UNIST), Ulsan 44919, Republic of Korea

*E-mails: kimds@unist.ac.kr (D. S. Kim), syy3@pusan.ac.kr (S. Y. Yoon), yescho@pusan.ac.kr (Y. R. Cho), shjin@pusan.ac.kr (S. H. Jin)

Materials: Fluorine-doped tin oxide on glass (FTO, sheets resistance 7 Ω sq^{-1}) was purchased from Asahi. The mesoporous TiO_2 (SC-HT040) paste was purchased from Share Chem. Ethanol (absolute, 99.9%) and diethyl ether (extra pure grade) were purchased from Duksan. Methylamine hydrochloride (MACl, ≥98%) was purchased from Acros Organics. The Spiro-OMeTAD was purchased from Lumtec. Titanium diisopropoxide bis(acetylacetonate), formamidine acetate salt (99%), hydriodic acid (HI, 57 wt% in water), 2-propanol (anhydrous, 99.5%), chlorobenzene (anhydrous, 99.8%), N,N-dimethylformamide (DMF, anhydrous 99.8%), N,N-dimethyl sulfoxide (DMSO, >99.5%), 2-methoxyethnaol (2-ME, anhydrous, 99.8%), and formic acid were procured from Sigma Aldrich. Lead iodide (PbI_2, 99.9985%) was purchased from TCI.

SYNTHESIS

Synthesis of 4-((*tert*-butyldimethylsilyl)oxy)aniline (1). 4-Aminophenol (5 g, 45.82 mmol) was solubilized in tetrahydrofuran (THF, 60 mL) and cooled to 0 °C with an ice bath. Then, imidazole (9.36 g, 137.45 mmol) and *tert*-butyldimethylsilyl chloride (TBSCl, 9.00 g, 59.56 mmol) was added at 0 °C under N_2 atmosphere. Afterwards, the solution was stirred 3 h at room temperature (RT). After that distilled water and the mixture was extracted with ethyl acetate (EA). The organic layer was dried over anhydrous Na_2SO_4. The solvents were evaporated under reduced pressure, and the crude product was purified by column chromatography on silica gel with EA : hexane = 1 : 5 (v/v) to afford the pure product as a yellow oil (9.46 g, 92%). ^{1}H NMR (400 MHz, $CDCl_3$): δ [ppm] 6.25-6.50 (d, 2H), 6.44-6.42 (d, 2H), 3.24 (s, 2H), 0.82 (s, 9H), 0.00 (s, 6H).

Synthesis of *N*-(4-((*tert*-butyldimethylsilyl)oxy)phenyl)-3-fluoro-4-methoxyaniline (2). Compound 1 (5 g, 22.38 mmol) and 4-bromo-2-fluoro-1-methoxybenzene (3.03 mL, 23.50 mmol) in anhydrous toluene (40 mL) was purged with N_2 for 20 min. Then, tris(dibenzylideneacetone)dipalladium ($Pd_2(dba)_3$) (1.03 g, 1.12 mmol), tri-*tert*-butylphosphonium

tetrafluoroborate (0.65 g, 2.24 mmol) and sodium *tert*-butoxide (6.45 g, 67.15 mmol) were added and the solution was refluxed for overnight under N_2 atmosphere. After cooling to RT, distilled water and the mixture was extracted with methylene chloride (MC). The organic layer was dried over anhydrous Na_2SO_4. The solvents were evaporated under reduced pressure, and the crude product was purified by column chromatography on silica gel with MC : hexane = 7 : 10 (v/v) to afford the pure product as a pale brown solid (5.62 g, 72%). ^{1}H NMR (400 MHz, DMSO-D_6): δ [ppm] 7.58 (s, 1H), 6.84-6.80 (t, 1H), 6.75-6.72 (m, 2H), 6.60-6.59 (d, 1H), 6.58-6.55 (m, 2H), 6.54-6.50 (m, 1H), 3.57 (s, 3H), 0.76 (s, 9H), 0.02 (s, 6H).

Synthesis of N^2,$N^{2'}$,N^7,$N^{7'}$-tetrakis(4-((*tert*-butyldimethylsilyl)oxy)phenyl)-N^2,$N^{2'}$,N^7,$N^{7'}$-tetrakis(3-fluoro-4-methoxyphenyl)-9,9'-Spirobi[fluorene]-2,2',7,7'-tetraamine (3). 2,2',7,7'-Tetrabromo-9,9'-spirobi[fluorene] (2 g, 3.16 mmol) and compound 2 (5.50 g, 15.82 mmol) in anhydrous toluene (40 mL) was purged with N_2 for 20 min. Then, $Pd_2(dba)_3$ (0.09 g, 0.10 mmol), tri-*tert*-butylphosphonium tetrafluoroborate (0.07 g, 0.25 mmol) and sodium *tert*-butoxide (0.91 g, 9.49 mmol) were added and the solution was refluxed for overnight under N_2 atmosphere. After cooling to RT, distilled water and the mixture was extracted with MC. The organic layer was dried over anhydrous Na_2SO_4. The solvents were evaporated under reduced pressure, and the crude product was purified by column chromatography on silica gel with MC : hexane = 3 : 5 (v/v) to afford the pure product as a white solid (1.13 g, 77%). ^{1}H NMR (400 MHz, DMSO-D_6): δ [ppm] 7.37-7.35 (d, 4H), 6.89-6.84 (t, 4H), 6.69-6.67 (d, 8H), 6.61-6.56 (m, 14H), 6.54-6.53 (d, 2H), 6.50-6.48 (d, 4H), 6.03 (d, 4H), 3.63 (s, 12H), 0.77(s, 36H), 0.00 (s, 24H).

Synthesis of 4,4',4'',4'''-((9,9'-spirobi[fluorene]-2,2',7,7'-tetrayl)tetrakis((3-fluoro-4-methoxyphenyl)azanediyl))tetraphenol (4). Compound 3 (0.25 g, 0.15 mmol) was solubilized in THF (20 mL) and cooled to 0 °C with an ice bath. Then, tetra-n-butylammonium fluoride

(TBAF, 0.68 mL, 0.68 mmol) (1 M in THF) was added dropwise at 0 °C under N_2 atmosphere. Afterward the solution was stirred 3 h at RT. After that distilled water and the mixture was extracted with EtOAc. The organic layer was dried over anhydrous Na_2SO_4. The solvents were evaporated under reduced pressure, and the crude product was purified by column chromatography on silica gel with EA: hexane = 2 : 5 (v/v) to afford the pure product as a pink solid (0.14 g, 77%). ^{1}H NMR (400 MHz, DMSO-D_6): δ [ppm] 9.4 (s, 4H), 7.53-7.51 (d, 24H), 7.01-6.96 (t, 4H), 6.81-6.79 (d, 8H), 6.74-6.65 (m, 14H), 6.60-6.58 (d, 4H), 3.78 (s, 12H).

Synthesis of N^2,$N^{2'}$,N^7,$N^{7'}$-tetrakis(4-(allyloxy)phenyl)-N^2,$N^{2'}$,N^7,$N^{7'}$-tetrakis(3-fluoro-4-methoxyphenyl)-9,9'-Spirobi[fluorene]-2,2',7,7'-tetraamine (Spiro-mF-A). Compound 4 (0.57 g, 0.46 mmol) and K_2CO_3 (0.35 g, 2.53 mmol) in anhydrous acetonitrile (20 mL) was purged with N_2 for 20 min. Then, allyl bromide (0.22 mL, 2.53 mmol) was added and the solution was refluxed for overnight under N_2 atmosphere. After cooling to RT, distilled water and the mixture was extracted with EA. The organic layer was dried over anhydrous Na_2SO_4. The solvents were evaporated under reduced pressure, and the crude product was purified by column chromatography on silica gel with EA : hexane = 3 : 10 (v/v) to afford the pure product as a white solid (0.61 g, 95%). ^{1}H NMR (400 MHz, DMSO-D_6): δ [ppm] 7.53-7.51 (d, 4H), 7.01-6.97 (t, 4H), 6.89-6.83 (m, 16H), 6.75-6.73 (dd, 4H), 6.71-6.70 (dd, 4H), 6.62-6.59 (d, 4H), 6.23 (s, 4H), 6.07-5.97 (m, 4H), 5.40-5.35 (dd, 4H), 5.26-5.23 (dd, 4H), 4.51-4.50 (dd, 8H), 3.77 (s, 12H). ^{13}C NMR (100 MHz, DMSO-D_6): δ [ppm] 155.18, 153.22, 150.79, 149.79, 147.13, 143.32, 143.22, 141.21, 141.13, 140.31, 134.93, 134.12, 126.68, 121.93, 121.01, 119.89, 117.91, 116.46, 116.05, 115.04, 111.84, 111.64, 68.85, 65.43, 56.59.

Synthesis of N^2,$N^{2'}$,N^7,$N^{7'}$-tetrakis(3-fluoro-4-methoxyphenyl)-N^2,$N^{2'}$,N^7,$N^{7'}$-tetrakis(4-(prop-2-yn-1-yloxy)phenyl)-9,9'-Spirobi[fluorene]-2,2',7,7'-tetraamine (Spiro-mF-P).

Compound 4 (0.5 g, 0.40 mmol) and K_2CO_3 (0.26 g, 1.85 mmol) in anhydrous acetonitrile (20 mL) was purged with N_2 for 20 min. Then, propargyl bromide (0.21 mL, 1.85 mmol) (80 wt% in toluene) was added and the solution was refluxed for overnight under N_2 atmosphere. After cooling to RT, distilled water and the mixture was extracted with EA. The organic layer was dried over anhydrous Na_2SO_4. The solvents were evaporated under reduced pressure, and the crude product was purified by column chromatography on silica gel with EA : hexane = 3 : 10 (v/v) to afford the pure product as a white solid (0.54 g, 96%). ^{1}H NMR (400 MHz, DMSO-D_6): δ [ppm] 7.57-7.54 (d, 4H), 7.04-6.99 (t, 4H), 6.90 (s, 16H), 6.78-6.75 (dd, 4H), 6.74-6.70 (dd, 4H), 6.64-6.62 (d, 4H), 6.23 (d, 4H), 4.76 (d, 8H), 3.79 (s, 12H), 3.56 (t, 4H). ^{13}C NMR (100 MHz, DMSO-D_6): δ [ppm] 154.11, 153.23, 150.79, 149.79, 147.12, 143.48, 143.37, 141.12, 141.04, 140.89, 134.98, 126.46, 122.03, 121.10, 120.19, 116.49, 116.28, 115.07, 112.11, 111.91, 79.68, 78.74, 65.43, 56.62, 56.10.

Synthesis of 4-(vinyloxy)aniline (5). 4-Aminophenol (5 g, 45.82 mmol), Cs_2CO_3 (11.9 g, 137.45 mmol) and CaC_2 (17.62 g, 274.90 mmol) in anhydrous DMSO (80 mL) and H_2O (7 vol%) were added and the solution was refluxed for 16 h under N_2 atmosphere. After cooling to RT, distilled water and the mixture was extracted with EA. The organic layer was dried over anhydrous Na_2SO_4. The solvents were evaporated under reduced pressure, and the crude product was purified by column chromatography on silica gel with EA : hexane = 3 : 10 (v/v) to afford the pure product as a brown oil (4.84 g, 78%). ^{1}H NMR (400 MHz, DMSO-D_6): δ [ppm] 6.88-6.84 (m, 2H), 6.69-6.65 (dd, 2H), 6.62-6.57 (dd, 1H), 4.64-4.6 (dd, 1H), 4.32-4.30 (dd, 1H), 3.56 (s, 2H).

Synthesis of 3-fluoro-4-methoxy-*N*-(4-(vinyloxy)phenyl)aniline (6). Compound 5 (0.5 g, 3.70 mmol) and 4-bromo-2-fluoro-1-methoxybenzene (0.48 mL, 3.74 mmol) in anhydrous toluene (40 mL) were purged with N_2 for 20 min. Then, $Pd_2(dba)_3$ (0.17 g, 0.18 mmol), tri-*tert*-butylphosphonium tetrafluoroborate (0.11 g, 0.37 mmol) and sodium *tert*-butoxide (0.53 g, 5.55

mmol) were added and the solution was refluxed for overnight under N_2 atmosphere. After cooling to RT, distilled water and the mixture was extracted with MC. The organic layer was dried over anhydrous Na_2SO_4. The solvents were evaporated under reduced pressure, and the crude product was purified by column chromatography on silica gel with MC : hexane = 3 : 10 (v/v) to afford the pure product as a brown oil (0.73 g, 76%). ^{1}H NMR (400 MHz, DMSO-D_6): δ [ppm] 7.00-6.94 (m, 4H), 6.92-6.88 (t, 1H), 6.85-6.81 (dd, 1H), 6.74-6.71 (m, 1H), 6.65-6.60 (dd, 1H), 5.44 (s, 1H), 4.72-4.69 (dd, 1H), 4.40-4.38 (dd, 1H), 3.88 (s, 3H).

Synthesis of N^2,$N^{2'}$,N^7,$N^{7'}$-tetrakis(3-fluoro-4-methoxyphenyl)-N^2,$N^{2'}$,N^7,$N^{7'}$-tetrakis(4-(vinyloxy)phenyl)-9,9'-Spirobi[fluorene]-2,2',7,7'-tetraamine (Spiro-mF-V).

2,2',7,7'-Tetrabromo-9,9'-Spirobi[fluorene] (0.2 g, 0.32 mmol) and compound 6 (0.38 g, 1.46 mmol) in anhydrous toluene (30 mL) was purged with N_2 for 20 min. Then, $Pd_2(dba)_3$ (14 mg, 0.02 mmol), tri-*tert*-butylphosphonium tetrafluoroborate (9 mg, 0.03 mmol) and sodium *tert*-butoxide (0.18 g, 1.90 mmol) were added and the solution was refluxed for overnight under N_2 atmosphere. After cooling to RT, distilled water and the mixture was extracted with EA. The organic layer was dried over anhydrous Na_2SO_4. The solvents were evaporated under reduced pressure, and the crude product was purified by column chromatography on silica gel with EA : hexane = 1 : 5 (v/v) to afford the pure product as a white solid (0.72 g, 69%). ^{1}H NMR (400 MHz, DMSO-D_6): δ [ppm] 7.60-7.58 (d, 4H), 7.04-7.00 (t, 4H), 6.95-6.88 (m, 16H), 6.83-6.78 (m, 8H), 6.75-6.74 (dd, 4H), 6.72-6.71 (d, 4H), 6.26 (d, 4H), 4.72-4.68 (dd, 4H), 4.46-4.44 (dd, 4H), 3.79 (s, 12H). ^{13}C NMR (100 MHz, DMSO-D_6): δ [ppm] 153.25, 152.56, 150.81, 149.79, 148.85, 146.98, 143.71, 143.60, 142.67, 140.84, 140.76, 135.33, 125.91, 122.65, 121.25, 120.44, 118.15, 117.08, 115.05, 112.39, 112.20, 95.48, 65.42, 56.58.

Synthesis of $FAPbI_3$: Formamidinium iodide (FAI) was synthesized as previously reported

elsewhere.[1] Briefly, formamidine acetate (25 g) was mixed with HI (50 mL) in a 250 mL round-bottomed flask under vigorous stirring. The powder with light-yellow color was synthesized after evaporating the solvent at 80℃ for 1h under vacuum conditions. The resultant powder was redissolved in ethanol and precipitated using diethyl ether. This procedure was repeated generally three times until white power was finally obtained. The white powder was recrystallized from a mixed ethanol and diethyl ether solution (1:1, v/v) in a refrigerator. The final white powder was collected with a glass filter and dried at room temperature for 24 h. $FAPbI_3$ black powder was synthesized as reported previously.[2] In detail, PbI_2 and FAI (1:1 molar ratio) were dissolved in 2ME (0.8 M) and then filtered using a polyvinylidene fluoride filter with 0.45 μm pore size. The filtered solution was placed in a flask incubated in an oil bath at 120 °C for 1 h under slow stirring. The resulting black powder was filtered using a glass filter and dried at 60 °C for 24 h.

Fabrication of PSCs: We fabricated all substrates using FTO glass from Asahi. The FTO glasses were washed using RCA-2 (H_2O_2/HCl/H_2O = 5:1:1) process for 10 min in an ultrasonic bath to remove impurities. And the substrates are washed with acetone and IPA for 10 min each. For fabricating of the electron transporting layer, which is the compact TiO_2 (c-TiO_2) layer, 60 mL of a titanium diisopropoxide bis(acetylacetonate)/ethanol (1:10, v/v) solution was deposited by spray pyrolysis method at 450 ℃. After finishing the spray pyrolysis process, the substrates were stored at 450 ℃ for 1 h and slowly cooled to RT. A mesoporous TiO_2 (mp-TiO_2, ~50 nm size of TiO_2) layer was deposited on the c-TiO_2 layer by spin coating at 3000 rpm. for 50 s. The mp-TiO_2 paste was dispersed in 2ME/terpineol (78:22, w/w) at a concentration of 17%. The resulting substrates were heated at 500 ℃ on a hotplate for 1 h to remove organic compounds and then slowly cooled down to 150 ℃. For Li treatment on the mp-TiO_2 substrate, lithium carbonate (Li_2CO_3) solution (0.5 mg/mL) with water was spin coated at 3,000 rpm and sintered at 500 °C for 1 h. Before coating

the perovskite film, the substrate was treated with argon and oxygen mixed plasma for 5 min. The perovskite precursor solution was prepared by dissolving $FAPbI_3$ (1550 mg) and MACl (60 mg) with DMF/DMSO (1 mL, 4:1, v/v). The precursor was filtered with a polyvinylidene fluoride filter (PVDF, 0.2 μm) and then 60 μL of the perovskite solution was spread on the surface of the substrates at 8000 rpm for 50 s. During the spinning, 1 mL of diethyl ether was dropped on the perovskite film at 10 s using a homemade pipette. The film was annealed at 150 ℃ for 10 min and 100 ℃ for 30 min on a hotplate. And then the substrates were cooled, octylammonium iodide/IPA solution (20 mM) was spin coated on the top of the perovskite film at 3000 rpm for 30 s. To fabricate the hole transporting layer, the various hole transporting material solutions were spin coated at 3000 rpm for 30 s. Spiro-OMeTAD solution in chlorobenzene (90 mg/mL) was doped with 4-*tert*-butylpyridine (*t*BP, 39 μL), Li-bis(trifluoromethanesulfonyl)imide (Li-TFSI, 23 μL) (520 mg/mL in acetonitrile) and tris(2-(1H-pyrazol-1-yl)-4-*tert*-butylpyridine)-cobalt(III)-tris(bis-(trifluoromethylsulfonyl) imide) (FK-209, 5 μL) solution (180 mg/mL in acetonitrile). For Spiro-mF-V, Spiro-mF-A, and Spiro-mF-P (30 mg/mL), *t*BP (36 μL), Li-TFSI (20 μL), and FK-209 (5 μL) solution were added to solution in toluene and spin coated using the same process. All these processes were carried out in an ambient environment at strictly controlled 25% RH and at 25 °C. Finally, the 100 nm thickness of the Au electrode was deposited using a thermal evaporation system.

Characterization

XPS and UPS measurements were performed using a Nexsa XPS system (ThermoFisher Scientific, UK) equipped with monochromatized Al K□ and He I radiations at $h\upsilon$ = 1486.6 eV for XPS and 21.22 eV for UPS with a base pressure of 2×10^{-7} to 2×10^{-8} Torr. The XRD was measured using PANalytical with EMPYREAN model; Optics incident beam path Bragg-Brentano HD, Anti-

scatter slit 1/2, and Divergence slit 2; Optics diffracted beam path PIXcel3D 1x1 detector. The perovskite solar cells were measured using a solar simulator (Newport-Oriel 94083 A, Class AAA) together with a Keithley source meter 2400 under ambient conditions (25% RH at 25 °C). Using a Si-reference cell certified by NREL for the light intensity was calibrated to 100 mW/cm^2. The J-V curves were measured under both forward and reverse scans using the shadow metal mask for a limited area to 0.0803 cm^2. External quantum efficiency (EQE) measurements were procured using a QEX7 system (PV Measurement, Inc.). Time-Resolved Photoluminescence (TRPL) measurements were obtained using PicoQuant FluoTime 300 (PicoQuant GmbH, Germany) equipped with a PDL 820 laser pulse driver. A pulsed laser diode (λ = 375 nm, pulse FWHM (full width at halfmaximum) < 70 ps, repetition rate 200 kHz to 40 MHz) was used to excite the sample. The AFM images were measured for the film roughness and morphologies by Scanning Probe Microscope of AFM5100N (Hitachi, Japan). SEM imaging were performed on a S-4800 instrument (Hitachi, Japan) at an accelerating voltage of 15.0 kV. The impedance response was measured over the range of 1 Hz to 1 MHz with oscillation amplitude of 15 mV under dark condition (Bio-Logic VMP-3). The experimental data were simulated using commercial Z-view software to estimate the values for each component of the corresponding equivalent circuits. Water contact angles were measured using a contact angle 101 measuring system (Plasma systems and materials, Korea).

SCLC Measurement

The hole mobility of the HTMs were measured by SCLC method using hole-only following device configuration ITO/PEDOT:PSS/HTMs/MoO_3 (5 nm)/Ag (100 nm). ITO glass substrate was sequentially washed with distilled water, acetone, and IPA. The substrates were treated with UV/ozone for 10 min. PEDOT:PSS was spin coated at 3000 rpm for 30 s and annealed at 150 °C

for 20 min. The HTM (30 mg/mL in toluene solution) were spin coated at 3000 rpm for 30 s. Then 5 and 100 nm-thick MoO_3 and Ag layer were evaporated onto the HTMs layer. The hole mobility (μ_h) were determined by fitting the dark current to the model of a single carrier SCLC, described by the equation:

$J = 9/8\ \varepsilon_0\varepsilon_r\mu V^2/d^3$

Where, J is the current, ε_0 is the permittivity of free space, ε_r is the relative permittivity of the material, d is the thickness of the HTM layer, V is the effective voltage.

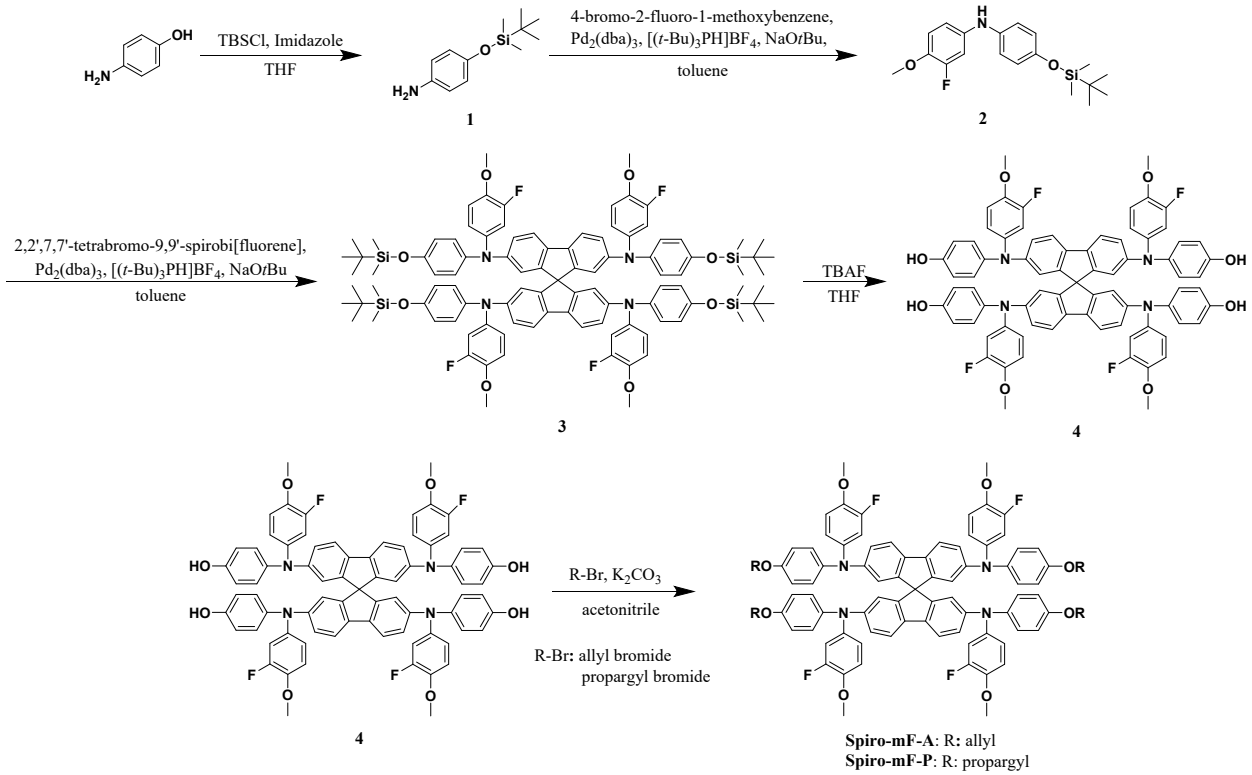

Fig. S1 Synthetic route of Spiro-mF-A and Spiro-mF-P.

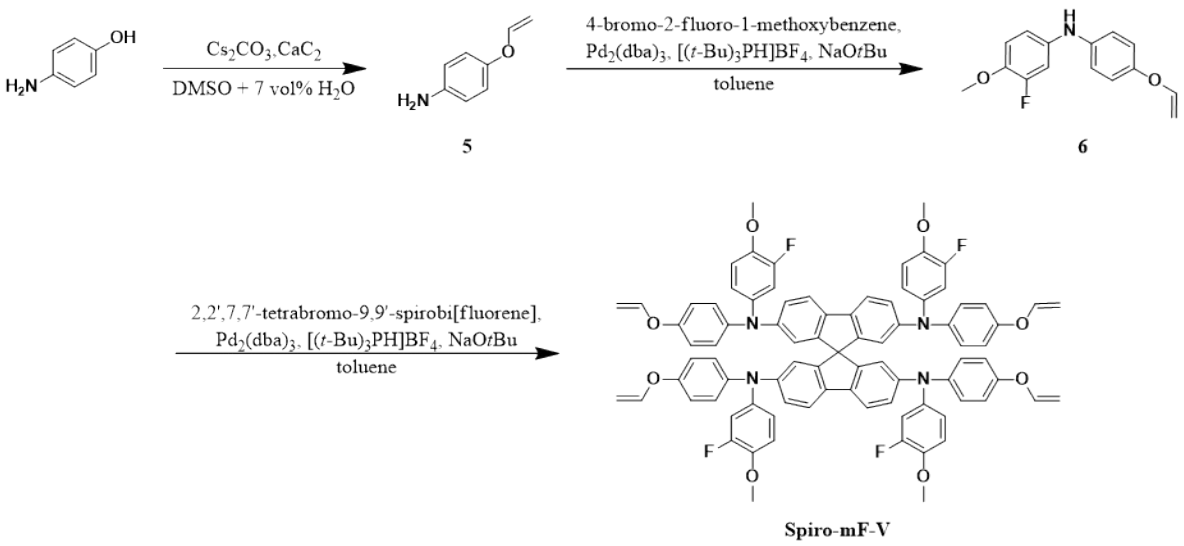

Fig. S2 Synthetic route of Spiro-mF-V.

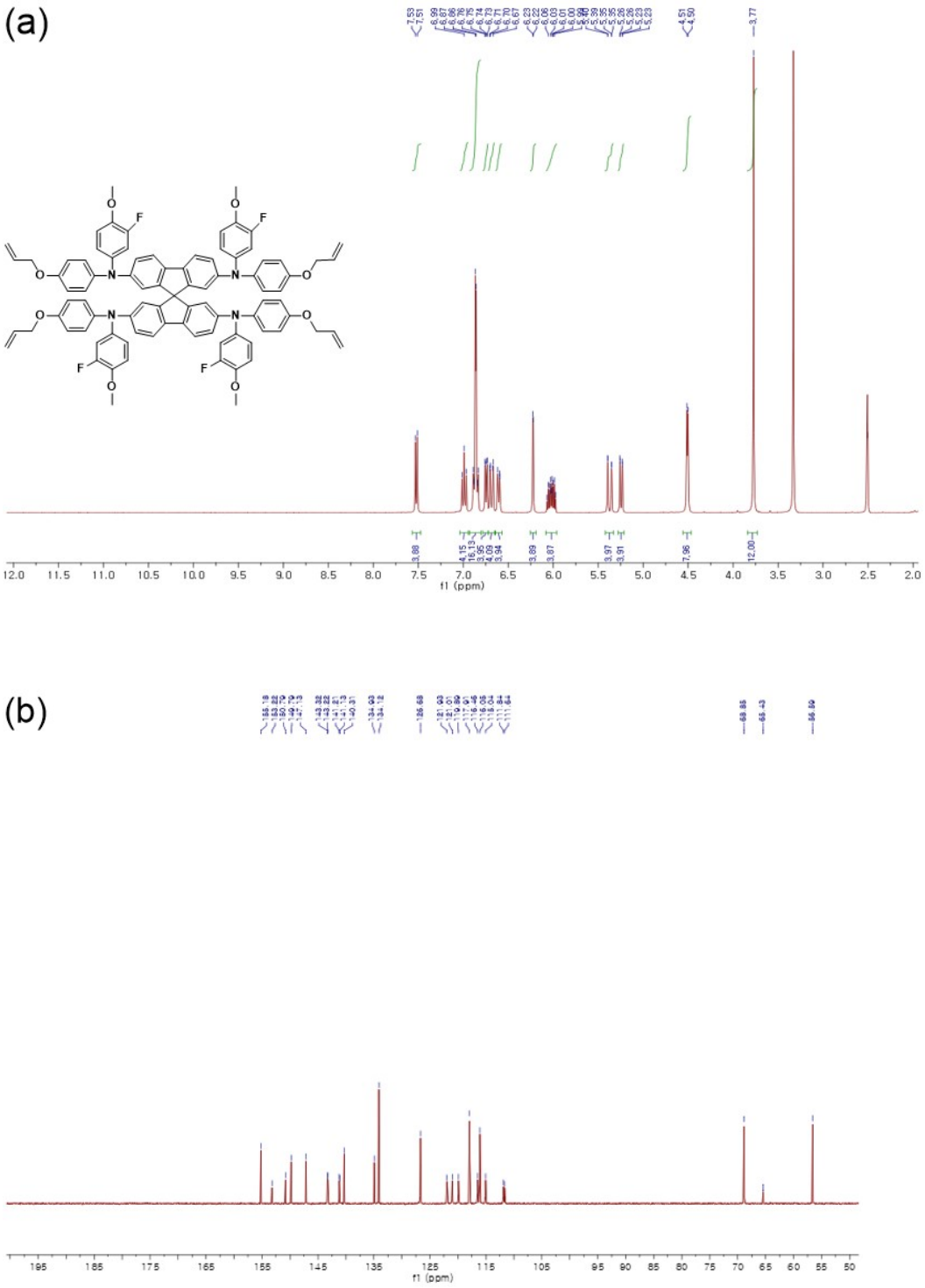

Fig. S3 (a) ^{1}H NMR and (b) ^{13}C NMR spectra of Spiro-mF-A.

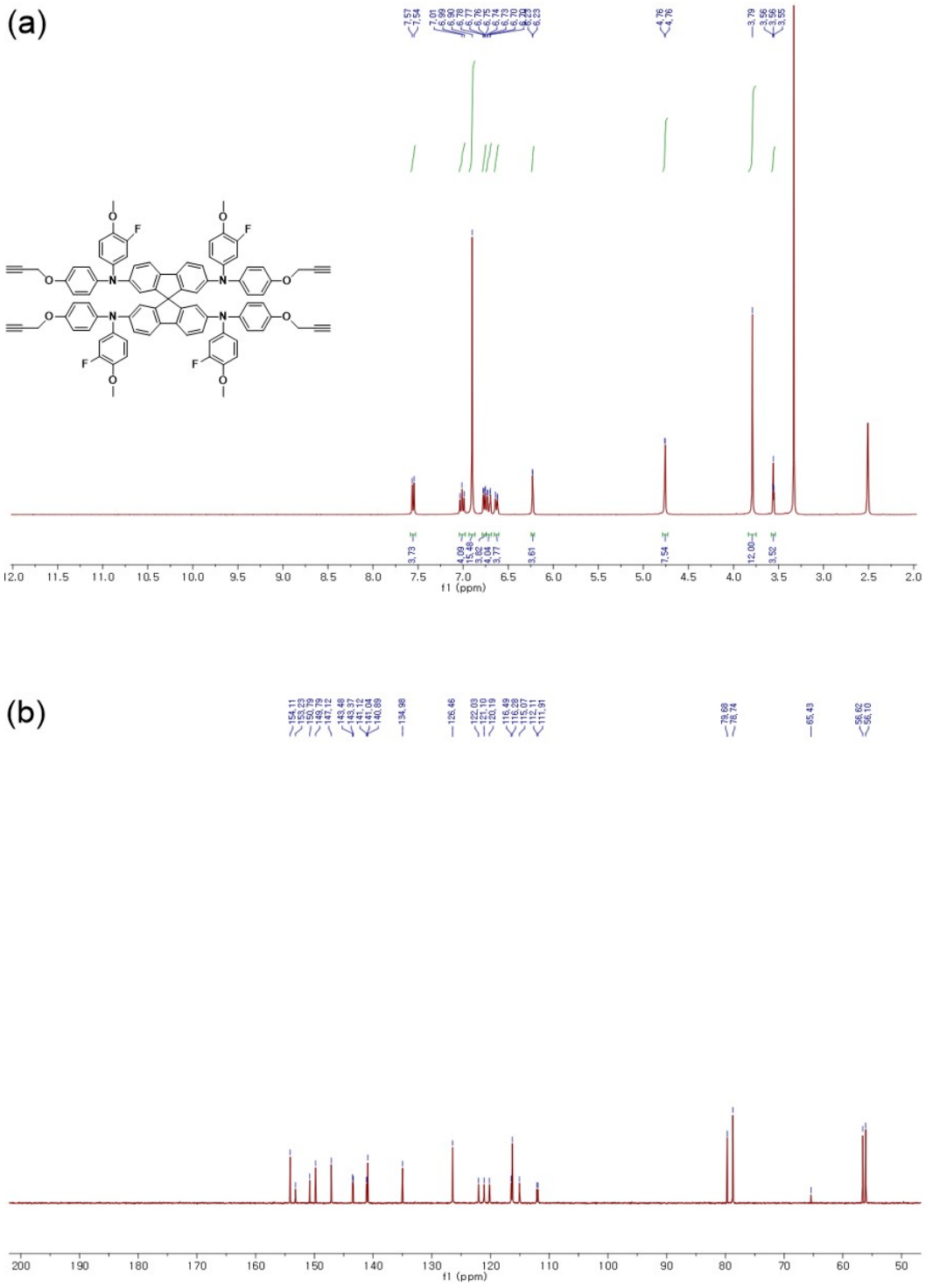

Fig. S4 (a) ^{1}H NMR and (b) ^{13}C NMR spectra of Spiro-mF-P.

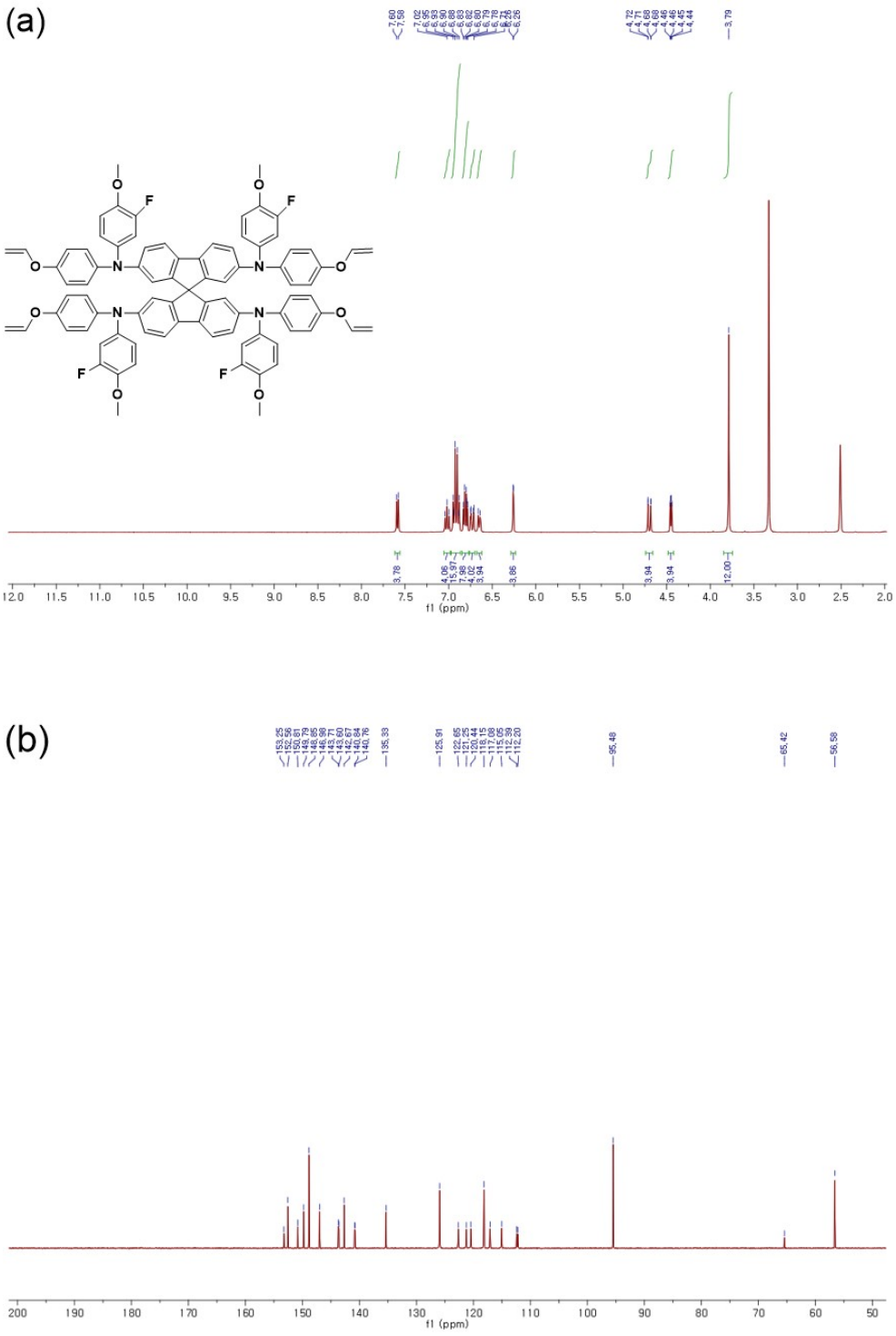

Fig. S5 (a) ^{1}H NMR and (b) ^{13}C NMR spectra of Spiro-mF-V.

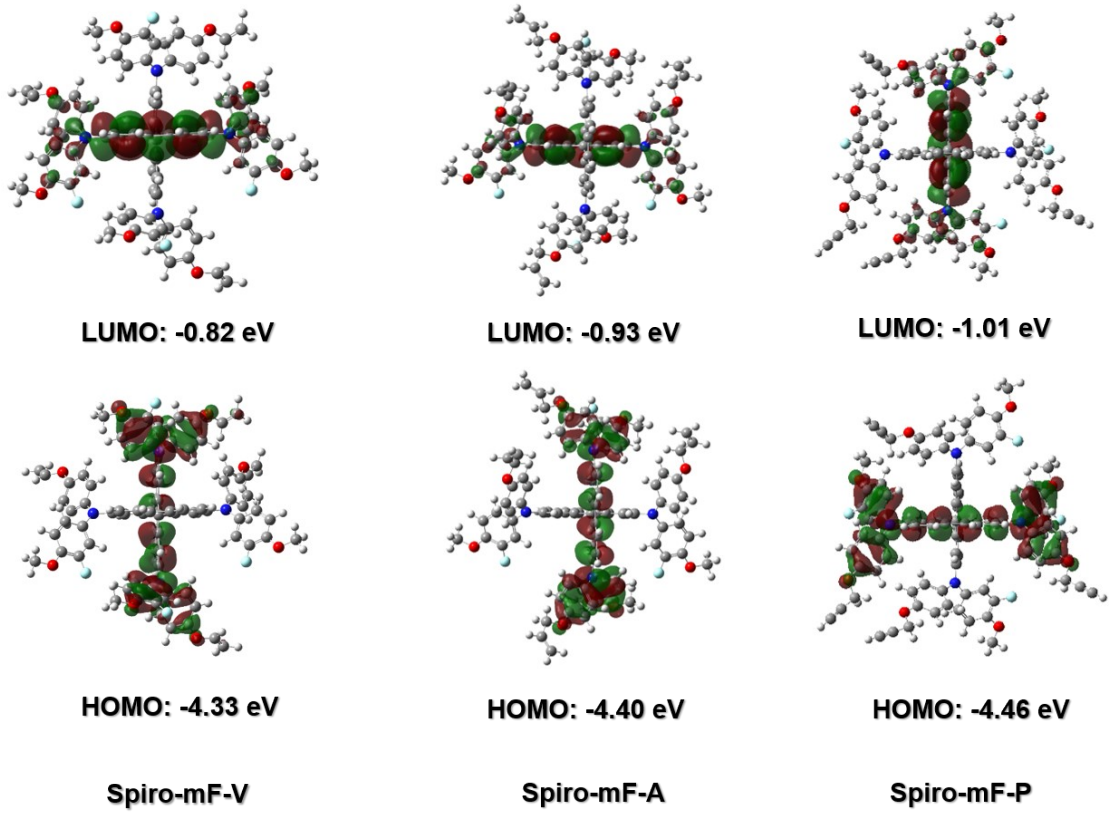

Fig. S6 DFT calculations of HOMO and LUMO of Spiro-mF-V, Spiro-mF-A, and Spiro-mF-P.

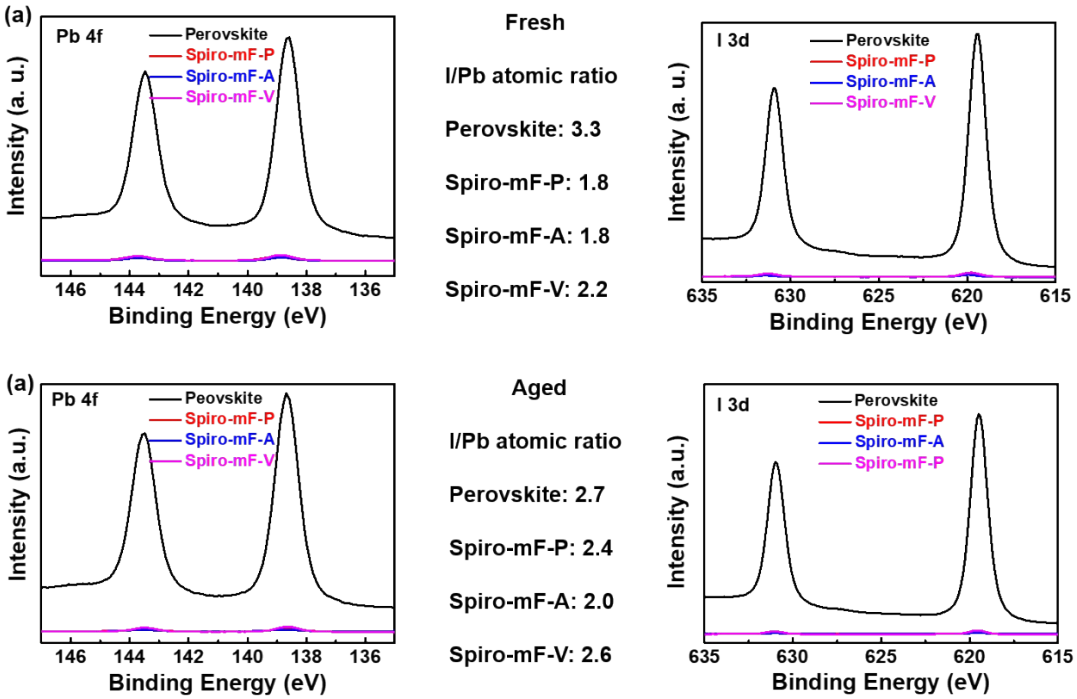

Fig. S7 Pb 4f and I 3d XPS spectra of (a) fresh and (b) aged (after 40 days in dry room condition) perovskite and HTMs-treated perovskite film.

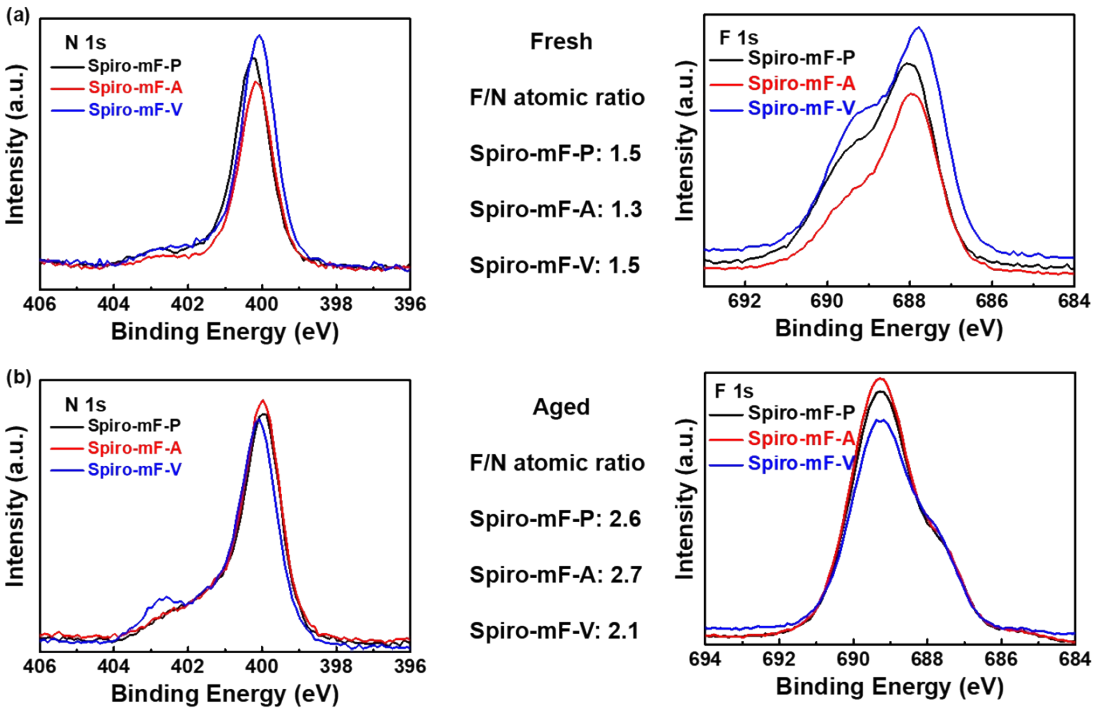

Fig. S8 N 1s and F 1s XPS spectra of (a) fresh and (b) aged (after 40 days in dry room condition) perovskite and HTMs-treated perovskite film.

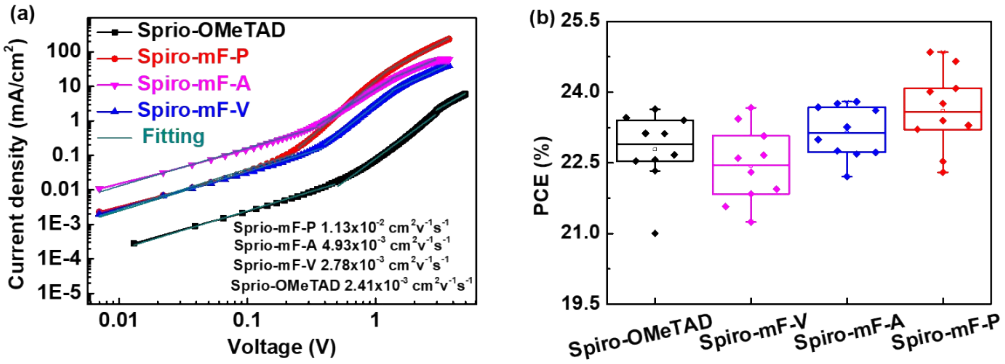

Fig. S9 (a) The hole mobility and (b) PCE distributions of doped Spiro-OMeTAD, Spiro-mF-V, Spiro-mF-A, and Spiro-mF-P.

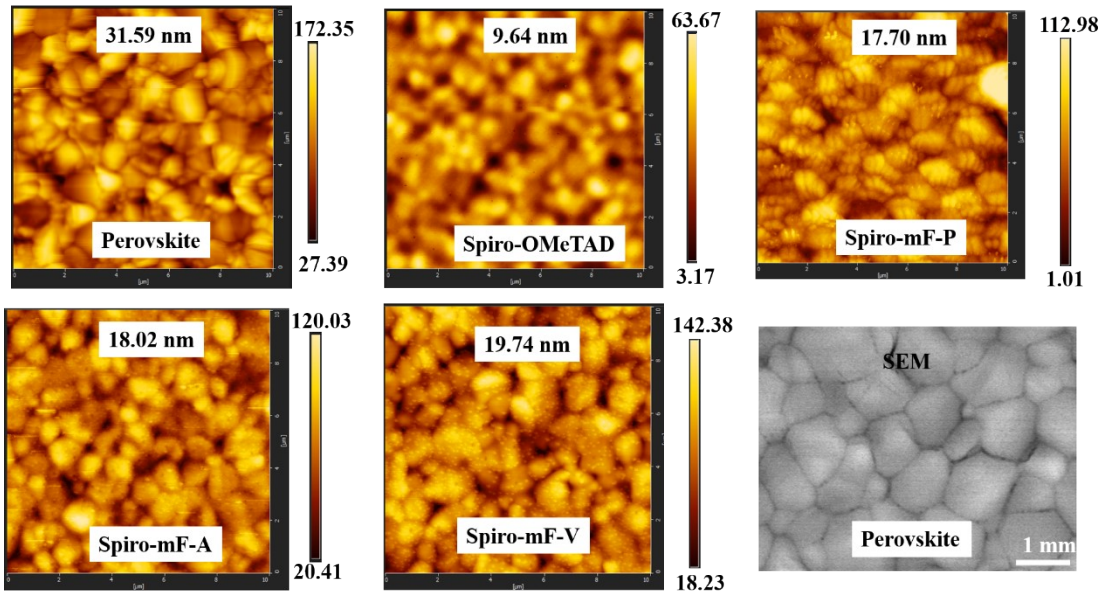

Fig. S10 The AFM of FTO/TiO_2/perovskite, FTO/TiO_2/perovskite/Spiro-OMeTAD, FTO/TiO_2/perovskite/ Spiro-mF-P, FTO/TiO_2/perovskite/Spiro-mF-A and FTO/TiO_2/perovskite/Spiro-mF-V films, and SEM of perovskite.

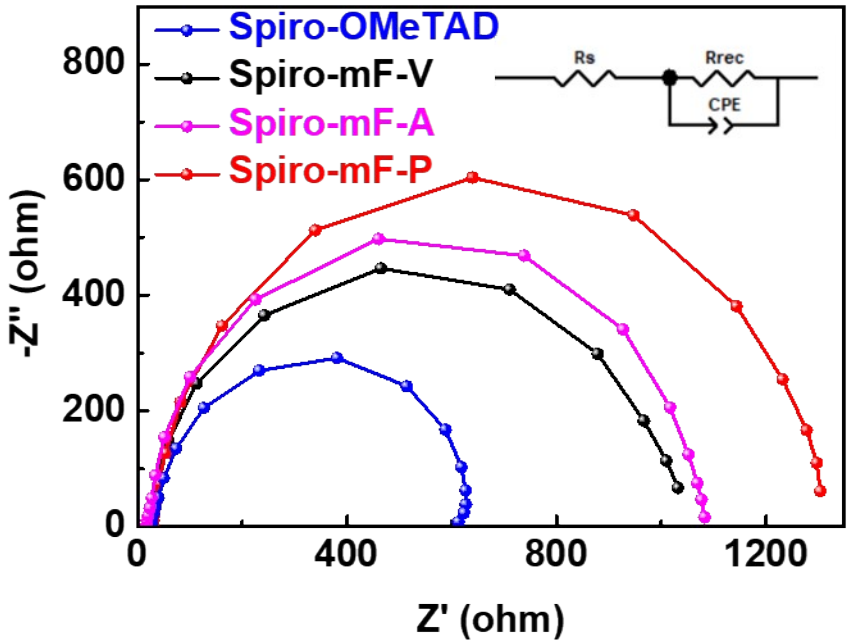

Fig. S11 (a) The Nyquist plots of different HTMs-based PSCs.

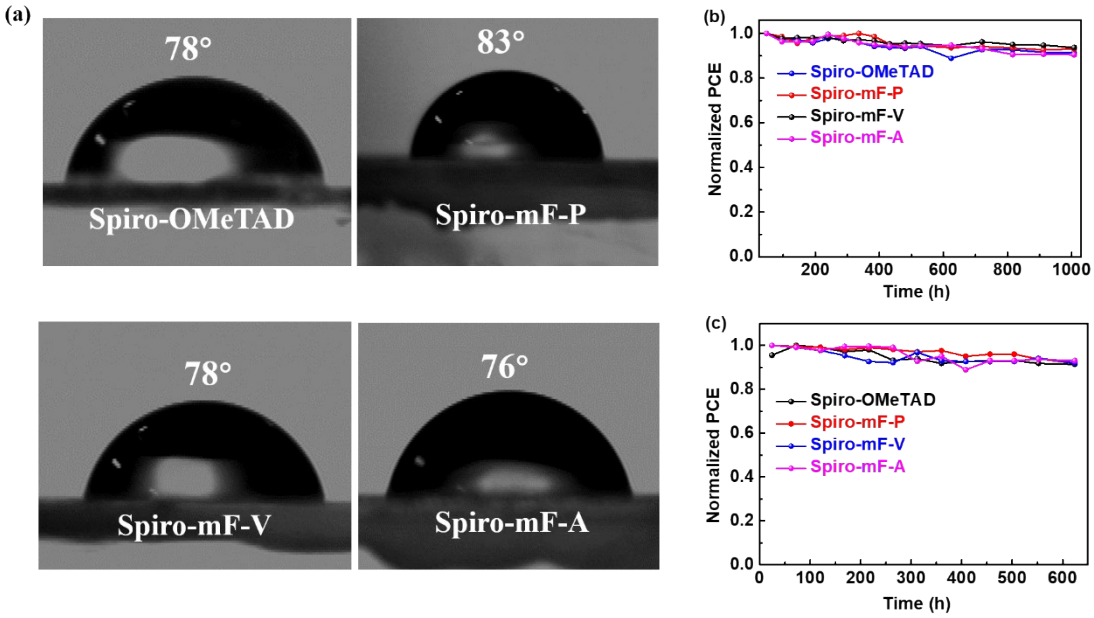

Fig. S12 (a) Water contact angles. (b) encapsulated (open-air) and (c) un-encapsulated (N_2) device stability of different HTMs-based PSCs.

Table S1 Thermal, optical and electrochemical properties of Spiro-OMeTAD, Spiro-mF-V, Spiro-mF-A, and Spiro-mF-P.

Material	Solution λ_{max} [a] [nm]	E_g^{opt} [b] [eV]	$E_{valance}$ [c] [eV]	High BE [d] [eV]	Work function (φ) [e] [eV]	HOMO [f] [eV]	LUMO [g] [eV]	T_g [h] [℃]	T_d [i] [℃]
Spiro-OMeTAD	310, 390	3.01	1.30	17.51	3.71	-5.01	-2.00	137	431
Spiro-mF-V	309, 384	2.95	1.54	17.61	3.61	-5.15	-2.20	142	416
Spiro-mF-A	307, 386	2.99	1.43	17.32	3.90	-5.33	-2.34	146	423
Spiro-mF-P	307, 385	3.00	2.19	18.04	3.18	-5.37	-2.37	144	425

[a] Measured in $CHCl_3$ solution with a concentration of 10^{-5} mol L^{-1}. [b] Optical band gap (E_g^{opt}), calculated from the onset of UV-Vis spectra, $E_g^{opt} = 1240/\lambda$. [c] Derived from valence band. [d] Derived from UPS spectra energy cutoff. [e] Work function was calculated by the equation $\varphi = 21.22 - (E_{cutoff} - E_f)$. [f] Highest occupied molecular orbital (HOMO) level was derived from the equation: $HOMO = -(E_{valence} + WF)$. [g] LUMO value was calculated from HOMO value, $LUMO = HOMO + E_g^{opt}$. [h] DTA with a heating rate of 10 ℃ min^{-1} under N_2 [i] Temperature with 5% mass loss was measured by TGA with a heating rate of 10 ℃ min^{-1} under N_2.

Table S2. Photovoltaic parameters of PSCs with different concentration HTMs at different thicknesses under Simulated Air Mass (AM) 1.5G at 100 mW/cm^2.

HTMs	Concentration [mg/ml]	Thickness [nm]	V_{oc} [V]	J_{sc} [mA/cm^2]	FF [%]	PCE [%]
Spiro-mF-V	10	35±5	0.95	23.41	69.80	15.55
	30	60±5	1.16	25.63	79.57	23.70
	50	100±5	1.11	25.36	76.02	21.47
Spiro-mF-A	10	35±5	0.98	23.74	68.59	15.88
	30	60±5	1.16	25.91	79.46	23.80
	50	100±5	1.12	25.82	76.37	22.03
Spiro-mF-P	10	35±5	1.02	24.61	70.28	17.62
	30	60±5	1.17	25.94	81.62	24.85
	50	100±5	1.11	25.96	79.94	23.01

Table S3 Spiro-derivative HTMs in perovskite solar cells.

HTM	Solvent	Concentration [mg ml^{-1}]	Efficiency [%]	Year	Reference
Spiro-mF-P	Toluene	30	**24.85**	2023	This Work
Spiro-mF-A	Toluene	30	**23.80**	2023	This Work
Spiro-mF-V	Toluene	30	**23.70**	2023	This Work
Spiro-Naph	Chlorobenzene	90.9	24.43	2022	3
Spiro-carbazole	Chlorobenzene	30	22.01	2022	4
Spiro-OMeTAD	Chlorobenzene	90	25.8	2021	5
SC	Chlorobenzene	46.3	21.76	2021	6
Spiro-PTZ	Chlorobenzene	26.76	18.36	2021	7
ST	Chlorobenzene	46.3	18.18	2021	6
Spiro-POZ	Chlorobenzene	17.52	18.14	2021	7
Spiro-mF	Chlorobenzene	90.9	24.82	2020	8
Spiro-oF	Chlorobenzene	90.9	24.50	2020	8
Spiro-TTB	Chlorobenzene	5	18.38	2020	9
Spiro-MeTAD	Chlorobenzene	40.60	17.2%	2020	10
Spiro-OMeIm	Chlorobenzene	128.4	17.1	2020	11
Spiro-TAD	Chlorobenzene	5	16.23	2020	9
Spiro-OPrTAD	Chlorobenzene	1449.85	16.86	2019	12
Spiro-OEtTAD	Chlorobenzene	1337.64	20.16	2019	12
Spiro-OBuTAD	Chlorobenzene	1562.06	19.04	2019	12
Spiro-tBuBED	Chlorobenzene	50	18.6	2019	13
Dm	Chlorobenzene	90.9	23.2	2018	14
2,4-Spiro-OMeTAD	Chlorobenzene	83	17.2	2018	15
X62	Chlorobenzene	15.95	15.9	2018	16
3,4-Spiro- OMeTAD	Chlorobenzene	83	9.1	2018	15
X61	Chlorobenzene	15.95	8	2018	16
X55	Chlorobenzene	72.75	20.8	2017	17
X54	Chlorobenzene	72.75	13.6	2017	17
Spiro-027	Chlorobenzene	72.3	16.60	2016	18
Sfx-MeOTAD	Chlorobenzene	85	12.4	2016	19
Spiro-CPDT	Chlorobenzene	46.62	13.4	2015	20
po-Spiro-OMeTAD	Toluene	12.25	16.7	2014	21
pm-Spiro-OMeTAD	Toluene	12.25	13.9	2014	21

Table S4 The eco-friendly solvent for the HTMs in perovskite solar cells.

HTM	Solvent	Efficiency [%]	Year	Reference
Spiro-mF-P	Toluene	**24.85**	2023	This work
Spiro-mF-A	Toluene	**23.80**	2023	This work
Spiro-mF-V	Toluene	**23.70**	2023	This work
Spiro-OMeTAD	Tetrahydrofuran	21.02	2021	22
M1	Ethyl acetate	20.14	2021	23
Ad-PhOMeTAD	Toluene	18.69	2021	24
M0	Ethyl acetate	18.32	2021	23
alkoxy-PTEG	2-methyl anisole	21.2	2020	25
MPA-BT-CA	Ethanol	20.52	2020	26
alkoxy-PTEG	3-methylcyclohexanone	19.9	2020	25
F23	Tetrahydrofuran	17.60	2020	27
asy-ranPBTBDT	2-methyl anisole	13.1	2020	28
AZO-IV	Toluene	11.62	2020	29
AZO-III	Toluene	9.77	2020	29
Spiro-OMeTAD	o-Xylene	15.2	2018	30
Spiro-OMeTAD	p-Xylene	14.1	2018	30
Spiro-OMeTAD	Toluene	14.0	2018	30
Spiro-OMeTAD	Phenetole	13.9	2018	30
Spiro-OMeTAD	Anisole	11.3	2018	30
Asy-PBTBDT	2-methylanisole	20.0	2017	31
Spiro-OMeTAD	Ethyl acetate	19.43	2017	32
po-Spiro-OMeTAD	Toluene	16.7	2014	21
pm-Spiro-OMeTAD	Toluene	13.9	2014	21

References

1. N. J. Jeon, J. H. Noh, W. S. Yang, Y. C. Kim, S. C. SRyu, J. W. Seo and S. I. Seok, *Nature*, 2015, **517**, 476–480.
2. M. Kim, T. K. Lee, I. W. Choi, H. W. Choi, Y. Jo, J. Lee, G.-H. Kim, S. K. Kwak and D. S. Kim, *Sustain. Energy Fuels*, 2020, **4**, 3753-3763.
3. M. Jeong, I. W. Choi, K. Yim, S. Jeong, M. Kim, S. J. Choi, Y. Cho, J.-H. An, H.-B. Kim, Y. Jo, S.-H. Kang, J.-H. Bae, C.-W. Lee, D. S. Kim and C. Yang, *Nat. Photonics*, 2022, **16**, 119-125.
4. M. Han, Y. Liang, J. Chen, X. Zhang, R. Ghadari, X. Liu, N. Wu, Y. Zhou, Y. Ding, M. Cai, H. Chen and S. Dai, *Chemsuschem*, 2022, **15**, e2022014.
5. H. Min, D. Y. Lee, J. Kim, G. Kim, K. S. Lee, J. Kim, M. J. Paik, Y. K. Kim, K. S. Kim, M. G. Kim, T. J. Shin and S. Il Seok, *Nature*, 2021, **598**, 444-450.
6. Z. Deng, M. He, Y. Zhang, F. Ullah, K. Ding, J. Liang, Z. Zhang, H. Xu, Y. Qiu, Z. Xie, T. Shan, Z. Chen, H. Zhong and C.-C. Chen, *Chem. Mater.*, 2020, **33**, 285-297.
7. J. Urieta-Mora, I. García-Benito, L. A. Illicachi, J. Calbo, J. Aragó, A. Molina-Ontoria, E. Ortí, N. Martín and M. K. Nazeeruddin, *Sol. RRL*, 2021, **5**, 2100650.
8. M. Jeong, C. I. Woo, E. M. Go, Y. Cho, M. Kim, B. Lee, S. Jeong, Y. Jo, H. W. Choi, J. Lee, J.-H. Bae, S. K. Kwak, D. S. Kim and C. Yang, *Science*, 2020, **369**, 1615–1620.
9. C. Wang, J. Hu, C. Li, S. Qiu, X. Liu, L. Zeng, C. Liu, Y. Mai and F. Guo, *Sol. RRL*, 2019, **4**, 1900389.
10. X. Sallenave, M. Shasti, E. H. Anaraki, D. Volyniuk, J. V. Grazulevicius, S. M. Zakeeruddin, A. Mortezaali, M. Grätzel, A. Hagfeldt and G. Sini, *J. Mater. Chem. A*, 2020, **8**, 8527-8539.
11. L. Hajikhanmirzaei, H. Shahroosvand, B. Pashaei, G. D. Monache, M. K. Nazeeruddin and M. Pilkington, *J. Mater. Chem. C*, 2020, **8**, 6221-6227.
12. F. Liu, S. Bi, X. Wang, X. Leng, M. Han, B. Xue, Q. Li, H. Zhou and Z. Li, *Sci. China Chem.*, 2019, **62**, 739-745.
13. P.-H. Lin, K.-M. Lee, C.-C. Ting and C.-Y. Liu, *J. Mater. Chem. A*, 2019, **7**, 5934-5937.
14. N. J. Jeon, H. Y. Na, E. H. Jung, T. Y. Yang, Y. G. Lee, G. J. Kim, H. W. Shin, S. I. Seok, J. M. Lee and J. W. Seo, *Nat. Energy*, 2018, **3**, 682-689.

15. M.-D. Zhang, D.-X. Zhao, L. Chen, N. Pan, C.-Y. Huang, H. Cao and M.-D. Chen, *Sol. Energy Mater. Sol. C.*, 2018, **176**, 318-323.
16. L. Wang, J. Zhang, P. Liu, B. Xu, B. Zhang, H. Chen, A. K. Inge, Y. Li, H. Wang, Y. B. Cheng, L. Kloo and L. Sun, *Chem. Commun.*, 2018, **54**, 9571-9574.
17. B. Xu, J. Zhang, Y. Hua, P. Liu, L. Wang, C. Ruan, Y. Li, G. Boschloo, E. M. J. Johansson, L. Kloo, A. Hagfeldt, A. K. Y. Jen and L. Sun, *Chem.*, 2017, **2**, 676-687.
18. Y. Shi, Y. Xue, K. Hou, G. Meng, K. Wang, R. Chi, F. Chen, H. Ren, M. Pang and C. Hao, *RSC Adv.*, 2016, **6**, 96990-96996.
19. M. Maciejczyk, A. Ivaturi and N. Robertson, *J. Mater. Chem. A*, 2016, **4**, 4855-4863.
20. M. Franckevičius, A. Mishra, F. Kreuzer, J. Luo, S. M. Zakeeruddin and M. Grätzel, *Mater. Horizons*, 2015, **2**, 613-618.
21. N. J. Jeon, H. G. Lee, Y. C. Kim, J. Seo, J. H. Noh, J. Lee and S. I. Seok, *J. Am. Chem. Soc.*, 2014, **136**, 7837-7840.
22. Z. Lin, J. Li, H. Li, Y. Mo, J. Pan, C. Wang, X.-L. Zhang, T. Bu, J. Zhong, Y.-B. Cheng and F. Huang, *Sci. China Mater.*, 2021, **64**, 2915–2925.
23. J. Huang, J. Yang, D. Li, H. Sun, M. Su, X. Ji, B. Li, B. Li, Q. Liao, D. Han, H. Yan, L. Niu, D. Wang and X. Guo, *J. Mater. Chem. C*, 2021, **9**, 8930-8938.
24. D. Fan, R. Zhang, Y. Li, C. Shan, W. Li, Y. Wang, F. Xu, H. Fan, Z. Sun, X. Li, M. Zhao, A. K. K. Kyaw, G. Li, J. Wang and W. Huang, *Front. Chem.*, 2021, **9**, 746365.
25. J. Lee, G. W. Kim, M. Kim, S. A. Park and T. Park, *Adv. Energy Mater.*, 2020, **10**, 1902662.
26. Y. Wang, Q. Liao, J. Chen, W. Huang, X. Zhuang, Y. Tang, B. Li, X. Yao, X. Feng, X. Zhang, M. Su, Z. He, T. J. Marks, A. Facchetti and X. Guo, *J. Am. Chem. Soc.*, 2020, **142**, 16632-16643.
27. H. Lu, B. He, Y. Ji, Y. Shan, C. Zhong, J. Xu, J. LiuYang, F. Wu and L. Zhu, *Chem. Eng. J.*, 2020, **385**, 123976.
28. H. I. Kim, J. Lee, M. J. Choi, S. U. Ryu, K. Choi, S. Lee, S. Hoogland, F. P. G. Arquer, E. H. Sargent and T. Park, *Adv. Energy Mater.*, 2020, **10**, 2002084.
29. J. Salunke, X. Guo, M. Liu, Z. Lin, N. R. Candeias, A. Priimagi, J. Chang and P. Vivo, *ACS Omega*, 2020, **5**, 23334-23342.

30. F. Isabelli, F. Di Giacomo, H. Gorter, F. Brunetti, P. Groen, R. Andriessen and Y. Galagan, *ACS Appl. Energy Mater.*, 2018, **1**, 6056-6063.
31. J. Lee, M. Malekshahi Byranvand, G. Kang, S. Y. Son, S. Song, G. W. Kim and T. Park, *J. Am. Chem. Soc.*, 2017, **139**, 12175-12181.
32. T. Bu, L. Wu, X. Liu, X. Yang, P. Zhou, X. Yu, T. Qin, J. Shi, S. Wang, S. Li, Z. Ku, Y. Peng, F. Huang, Q. Meng, Y.-B. Cheng and J. Zhong, *Adv. Energy Mater.*, 2017, **7**, 1700576.